COVID Infection Detection using Machine Learning Approach

Prita Patil[1], Vaibhav Narawade[2]

[1]Research Scholar,Department of Computer Engineering,
Ramrao Adik Institute of Technology, D Y Patil Deemed to be University, India,
prita.patil@gmail.com

[2]Research Scholar,Department of Computer Engineering,
Ramrao Adik Institute of Technology, D Y Patil Deemed to be University, India,
vaibhav.narawade@rait.ac.in

Abstract*: *Medical imaging serves a significant role in medical diagnosis & therapy. Also plays a role in medical applications. The motivation of this work to research the most difficult topic in medical image processing nowadays is locating an ROI (Region of Interest) that can be retrieved automatically or semi-automatically.The goal of the suggested concept is to facilitate a step-up in the preprocessing of radiology pictures to locate regions of interest (ROI) in diagnosing respiratory illness using Machine Learning approaches. In addition, the generalizability of the methods is challenged when a single dataset is used. Different datasets often include images of differing quality, which may originate from various machine kinds and represent the circumstances of the nations and locations from where they originate. In this study, it is proposed RDD_ROI (Respiratory Disease Detection_Region Of Interest) algorithm using a GLCM features & unsupervised K-means clustering technique to identify region of interest in the detection of respiratory disease like COVID, Pneumonia etc.Two large COVID-19 datasets (X-ray & CT scan image analysis with a patient) are used to evaluate the method. The analysis of images has been done based on seven different GLCM features like homogeneity, correlation, dissimilarity, contrast, entropy, energy. The results of features found that energy and correlation achieved 100%. These findings emphasized the importance of techniques designed to improve picture quality during COVID-19 identification in both image datasets, which would ultimately aid in the classification & detection of respiratory disease COVID based on analysis of the disease effect.

***Keywords*:Medical imaging data, Radiology images, Respiratory disease, COVID-19**

(Article history: Received: 3rd July 2023 and accepted 13th January 2024)

I. Introduction

Respiratory disease is also known as a lung problem. The main aspect is that this disease can be diagnosed, evaluated in several patterns, and assessed in different types of lung disease. The main examples of lung disease are pneumonia, COVID-19 and tuberculosis. In many countries, this disease, the main problem is the lack of radiologists [1]. The classification, identification and quantification of medical images can be made via DL (Deep Learning) & ML (Machine Learning) [2]. CXR (Chest X-Ray) images & chest radiography are processed for the medical image system for respiratory disease. Machine learning methods are achieving new trends to detect respiratory disease and set new parameters in the area of medical images. The computer aid diagnosis for respiratory disease contains many chest radiographs with large volumes of this type of image [3]. ML techniques for medical image application for respiratory disease detection have reached tremendous heights. In lung disease, interstitial and infiltrates changes is very predictive and limited [4]. There are several modern x-ray tools, mobile and fixed. The latest scanners have different techniques and two types of tube voltage, i.e., distribution of iodine.

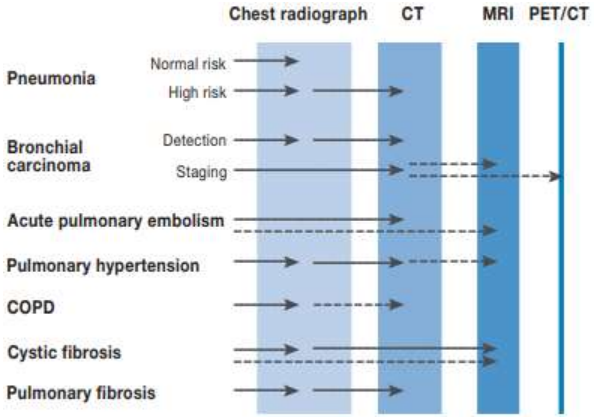

Fig. 1. Computed Tomography (CT), Chronic Obstructive Pulmonary Disease (COPD), Magnetic Resonance Imaging (MRI) and Positron Emission Tomography/CT (PET/CT) [5]

CT, MRI, PET/CT, & COPD are shown in Figure 1. Different types of medical photos may be mined for their numeric information. Main uses of machine learning algorithms for lung diseases called pulmonary nodule disease. Moreover, examining different machine learning with image processing and classification is based on several attributes [6]. The medical images dataset has different perspectives and uses CAD with machine learning algorithms like magnetic resonance imagining, chronic obstructive pulmonary disease and computed tomography.

These images analyzed with modest data with a machine learning algorithm can be more accurate than existing algorithms in the presence of unstructured data. The unstructured data can be classified into pdf, documents, images, videos, csv etc. The existing scholars have got chest x-ray images to deliver significant knowledge regarding covid-19 from CXR images which should come from every remote location in different countries. If it talks about covid-19, symptoms are cough, fatigue and fever.

On the other hand, headache, diarrhea, and sputum for excess [7]. In multiple cases, pneumonia that is leading to deprivation of oxygen. However, these symptoms lead to the body's kidney failure, heart attack and other serious diseases. Many reported cases demonstrate only mild symptoms, and existing studies show different symptoms of covid-19.

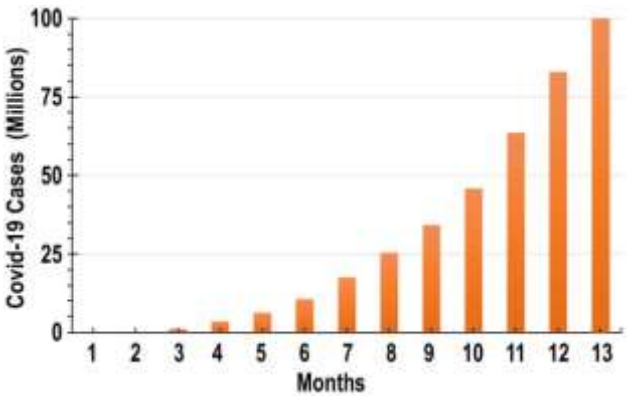

Fig. 2. Number of COVID-19 Cases across the Globe

The above figure 2 demonstrates different no. of covid cases across the world. This disease strikes lockdown, and social distancing steps were assessed in each affected country. This figure presents some cases with large distributions. The chest radiography requires periodic illness diagnosis and defining the significant outcomes in medical images, as it is a crucial step.

A lot of people are considering using machine learning (ML) in the medical imaging field. Potential uses include an entire range of medical imaging, from picture capture to analysis & prediction. Lack of access to adequate high-quality training data that has been meticulously curated and represents the problem space, with labels applied by experts, is a major barrier to the research, development, & clinical use of ML algorithms (for example, annotations). To train, verify, and test algorithms effectively, data curation is required for both supervised & unsupervised ML approach for picture segmentation to get a region of interest. Most research groups & businesses only have access to data from very small geographically focused samples. Algorithms with low utility and poor generalization result from the time-consuming and expensive data preparation procedure. In this article, the researchers discuss current limitations or research gaps in data preparation, describe the basic steps for preparing medical imaging data of CT scans & x-rays for further development in machine learning algorithm development, and investigate potential solutions to this issue.

The novel contribution of this work is outlined as follows:

- Identification of appropriate radiology image datasets is useful in studying the spread of respiratory disease infection.
- To investigate preprocessing techniques of radiology image data samples to obtain enhanced images in the medical field.
- To investigate and analyze the impact of radiological image data processing in detecting respiratory disease and fill the research gaps.
- Provide an unsupervised clustering approach to segment regions by locating ROI (Region of Interest) in detecting respiratory disease.
- To calculate the number of features of image datasets for each class.

This study provides an overview of lung cancer radiography pictures, a scan of the relevant literature, a definition of the problem, and a dataset utilized to solve this issue. Experiment results are presented, and a final remark & road map for the future is provided.

II. Related Work

In early 2020, different studies reported several shortcomings with RTPCR testing, incorporating a high false negative rate for detection purposes. The infected person involves several threats. Some public health datasets and methods identify accuracy, precision and number of treatments. This part shows a state-of-the-art method for existing methods on lung cancer via machine learning. This work provides a clear image of this approach's key method.

A. Respiratory Diseases

In 2022, N. Phukkaphan et al. [8] presented the worldwide health catastrophe brought on by the coronavirus COVID-19 epidemic that has spread to practically all nations. The fast spread of COVID-19 may be slowed down by using a diagnostic process that can rapidly & precisely identify the presence of infection. This work discusses our early investigation into using E-Nose (Electronic Nose) technology for COVID-19 infection detection. In this study, it reports on collecting and measuring human exhaled breaths for five minutes using commercial face masks from healthy volunteers, symptomatic COVID-19 patients, and asymptomatic COVID-19 patients in the closed system of an e-nose machine. The RT-PCR technique was used to validate the COVID-19 positive. According to the experiment, the total sensory response value may be used to define the strength of a human exhaled breath.

S. N. Syed Nor et al. [9] presented some technical suggestions to enhance the SPR sensor's accuracy, sensitivity, time response, & cost-saving techniques. Particular attention was paid to sensitivity enhancement elements such as a prism, support layer, nanomaterials, and type & form of optical fibres for early, rapid, & ultra-

sensitive viral infection detection. Therefore, a time-consuming molecular method is now the gold standard for diagnosing viral diseases. Detection of analyses and study of biomolecular interactions have extensively used the surface Plasmon resonance (SPR) phenomenon, which is also being researched as a rapid diagnostic technique for various viral illnesses.

S. Devaraj and M. N. Madian [10] presented the other pneumonia medical images and detected infection for multiple detection techniques. Data augmentation was employed in one of the investigations. Although it has been claimed that data augmentation improved classification accuracy, most works lacked data mining algorithms. Additional screening methods include X-rays and CT scans to identify an illness in the respiratory system. Due to COVID, pneumonitis, or other respiratory conditions, the categorization for visual evaluation in X-ray and CT pictures is complicated.

R. Anand et al. [11] explained persons and their cardiovascular sickness properly and made appropriate actions to avert heart absconds ahead of time. Alternate biological & real limits, such as age, sex, cholesterol level, blood pressure, pulse, and the location of the chest pain, may be used to estimate. The preparation & examination dataset was acquired from kaggle.com and consisted of fourteen different ascribes. AI-managed calculations often center on information, and the results demonstrate how well the suggested calculation approach compares to other options in terms of accuracy and precision.

X. Aggelides et al. [12] presented identifying and categorizing gestures connected to allergic rhinitis, and researchers propose a multidisciplinary Gesture Recognition case study. Among the most prevalent illnesses in the globe, allergic disorders, particularly allergic rhinitis, are largely unappreciated and significantly hinder everyday activities, including productivity at work.

B. Radiology Images Datasets

Data collected by medical imaging scanners like CT & MRI is referred to as "medical image data" & provides the foundation for a wide variety of medical visualization techniques & applications. There are nearly 1.35 million radiologic pictures in RadImageNet (RIN) collection, which span CT, MRI, & US modalities &11 anatomic areas also have been annotated by fellowship-trained & board-certified radiologists. This study aims to prove that pretraining with millions of radiologic photos is superior to ImageNet pictures for use in subsequent medical applications that rely on transfer learning. Patients who had a radiologic evaluation performed at an outpatient imaging facility between 2005 & 2020 were included in a retrospective analysis described in [13]. The study used the original research interpretation to backtrack and pull out the most important images & their labels. RIN models were trained using these photos and a random weight initiation. Using AUC for eight classification tasks & Dice scores for two segmentation challenges, RIN models were compared against ImageNet models. 1.35 million annotated medical pictures from 131 872 individuals who underwent CT, MRI, & the US for neurologic, musculoskeletal, gastrointestinal, oncologic, abdominal, endocrine, and pulmonary pathologic diseases comprise the RIN database. For TL (Transfer Learning) tasks on small datasets, including breast masses (US), thyroid nodules (US), meniscal tears (MRI), as well as anterior cruciate ligament injuries (MRI), RIN models outperformed ImageNet models significantly (P<.001) (9.4%, 4.0%, 4.8%, & 4.5% AUC improvements, respectively). RIN models demonstrated increased AUC (P<0.001) for bigger datasets, including pneumonia (chest radiography), intracranial hemorrhage (CT), COVID-19 (CT), and SARS-CoV-2 (CT), by 1.9 percent, 6.1 percent, 1.7 percent, and 0.9 percent, respectively. In addition, lesion localizations of the RIN models were enhanced by 64.6 percent & 16.4 percent, respectively, on thyroid and breast US datasets. Pretrained RIN models exhibited superior interpretability compared to ImageNet models, particularly for smaller radiologic datasets

C. .Machine Learning Approaches for Medical Imaging

The current AI revolution is based on ML, which has great potential for the clinical use of medical pictures [14][15][16]. It has been shown that ML performs comparably to medical specialists when diagnosing different illnesses using medical images [17]. Software applications are beginning to be approved for clinical usage [18][19]. ML might be key to attaining AI in medicine vision envisioned decades ago. Robert et al. [20] looked at 62 papers on ML for COVID but found none with practical use in the clinic.

DL is the most effective approach of ML, providing valuable analysis to examine a huge no. of CXR pictures that may have a significant influence on Covid-19 screening. In this study, R. Jain et al. [21] have adopted the PA perspective of CXR scans for covid-19 afflicted and healthy individuals. After cleaning the photos & augmenting the data, they compared the performance of CNN models depending on DL. They have compared the accuracy of Inception V3, ResNet, and Xception models. To evaluate the model's performance, 6432 CXR images were obtained from the Kaggle repository; 5467 were utilized for training & 965 for validation. In the result analysis, the Xception model detects CXR pictures with the best accuracy (97.97 percent) compared to other models.

This study focuses only on potential classification approaches for covid-19-infected individuals and makes no claim to medical accuracy.

Different datasets often include pictures of differing quality, which can originate from various CT scans that reflect the circumstances of nations and places from which they originate. P. Silva et al. [22] suggested an Efficient DL approach for screening COVID-19 via a voting-based method to overcome these two issues. Using a voting mechanism, images of certain patients are categorized as a

group in this method. The method is evaluated on two major patient-based COVID-19 CT analysis datasets. A cross-dataset analysis is also provided to assess models' resilience in a more realistic situation when data originates from various distributions. Cross-dataset study demonstrates that the generalization ability of DL models is insufficient for the task, as accuracy reduces from 87.68 percent to 56.16 percent under the best assessment scenario. These findings demonstrated that COVID-19 detection techniques in CT images must be greatly improved before they can be considered clinical alternatives and also that bigger & more varied dataset are required to test approaches in a realistic scenario

III. Research Gaps

Computer analysis of medical pictures research has great potential for improving patient health. Nonetheless, several systemic obstacles impede the advancement of the area, including data restrictions, biases, and research incentives, like optimizing for publication. This study examines obstacles to designing and evaluating techniques. By basing our research on evidence from literature & data difficulties, It demonstrates that possible biases might manifest at every stage. Computer analysis of medical pictures research has great potential for improving patient health.

Nonetheless, some systematic obstacles impede the advancement of the area, including data limitations, biases, and research incentives, like optimizing for publication. This study examines obstacles to designing & evaluating methods. By basing our research on evidence from scholarly literature & data difficulties, It demonstrates that possible biases might arise at every stage. The stakes are enormous, and there is an astounding amount of study on medical imaging ML. However, this expansion does not always result in clinical progress. The increased research output might be aligned with academic motivations rather than physicians' & patients' requirements. For instance, there may be an abundance of articles demonstrating advanced performance on benchmark data, nonetheless little progress in clinical problems.

Big labelled datasets, which might include millions of photos, have made it possible to solve difficult ML problems like natural image recognition in computer vision. Therefore, there is broad optimism that comparable advancements would be made in medical applications; algorithm development must address clinical issues expressed as discriminating challenges. DL has shown promise for nature image enhancement and has exceeded standard ML techniques in some applications. Deep learning applications in medical imaging include disease screening, such as analysing retinal fundus images and classifying brain cancer states and lung disease. Deep learning's ability to automatically extract the most relevant features for data interpretation and inference directly from annotated data has aided its rapid growth and widespread application in a variety of fields. However, this comes at the expense of necessitating a massive amount of data with expert annotations in order to train the DL model.

In practise, obtaining a large number of expert-annotated datasets in the medical image domain is difficult. To obtain annotation from medical images, experts such as physicians or radiologists who are busy with clinical duties must accurately label the medical images. Furthermore, unlike raw image analysis, where images can be easily captured using a standard camera, medical images such as CT, MRI, PET, and others are difficult and expensive to capture. As a result, the requirement for DL in medical image applications to generate generalizable learning from small datasets is becoming increasingly important.

It hopes to collect various research papers on ML in medical imaging with limited datasets in this Research Topic. Preprocessing data is critical for obtaining enhanced and segmented image datasets. We eagerly await reviews and research on advanced technology in the field.

IV. Material and Methods

Data availability and different methods used to perform preprocessing are explained in this section.

A. Dataset Availability

For this study, two medical imaging datasets are taken, and a brief detail about these two datasets, namely, CXR images & CT images dataset, are given below.

1) CXR images dataset

CXR (Covid-19 & Pneumonia) collection includes CXR pictures of Covid-19, Pneumonia, & normal patients. Dataset is arranged into two directories (train & test), and each folder has three subfolders (COVID19, PNEUMONIA, NORMAL). Figure 3 displays the sample pictures for Covid-19, Pneumonia, & normal.

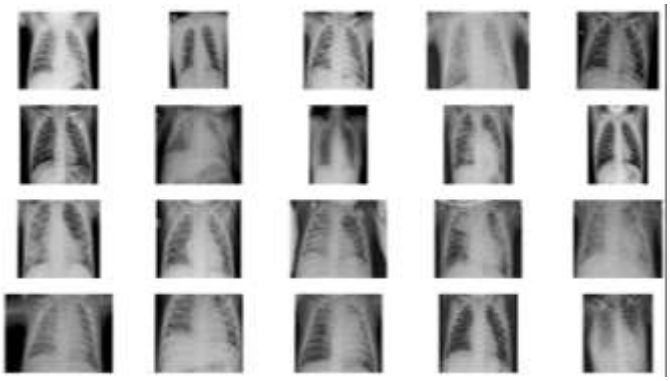

(a) Covid19 images

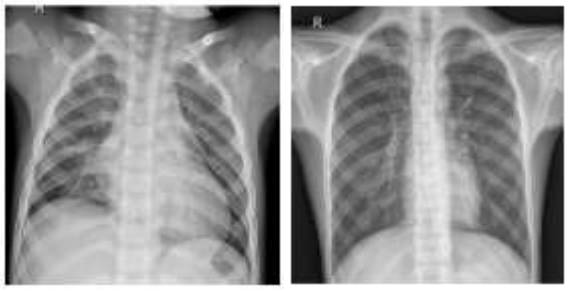

(b) Pneumonia images (c) Normal images

Fig. 3. Sample images of X-ray images

The dataset comprises 6432 X-ray pictures, with test data being 20 percent of the total images. This data set may be found at "https://www.kaggle.com/datasets/prashant268/chest-xray-covid19-pneumonia." Data distribution information for all three classes is shown below in table 1.

Table 1. Data Information of Chest X-Ray

Data	Covid19	Pneumonia	Normal	Total
Training	460	3418	1266	5144
Testing	116	855	317	1288

2) CT images dataset

Two datasets, namely, the SARS-CoV-2 and the CT-Scan datasets, have been considered. The first data is the CT-Scan dataset, which may be employed to classify and automatically detect COVID-19 on CT scans. COVID-19 Lung CT Scans CT Scan Dataset pertaining to COVID-19 and pictures were gathered from COVID19-related articles published on bioRxiv, medRxiv, JAMA, Lancet, NEJM, etc. CTs with COVID-19 abnormalities are chosen by reading the captions of the figure in published studies. The dataset contains a total of 746 CT scan total images. A CT-Scan dataset is available at: (https://www.kaggle.com/datasets/luisblanche/covidct?select=CT_COVID). Figure 4 shows a sample image of a CT scan.

The SARS-CoV-2 CT-scan dataset includes 2482 scans from 120 patients: 1252 scans from 60 SARS-CoV-2-infected patients (28 females and 32 males) and 1230 scan images from 60 patients were not infected with SARS-CoV-2 but were afflicted with other pulmonary diseases. The hospitals in Sao Paulo, Brazil, provided the data. The SARS-CoV-2 data set may be seen at "https://www.kaggle.com/datasets/plameneduardo/sarscov2-ctscan-dataset."

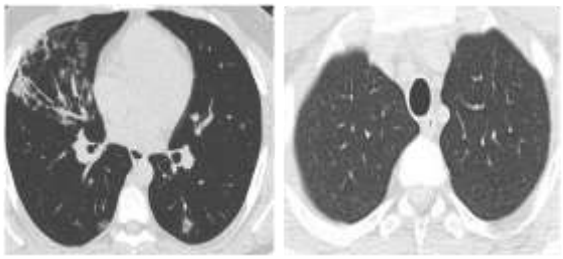

(a) Covid19 images (b) Non-Covid19 images

Fig. 4. Sample images of CT images

Table 2 represents the data distribution information for two datasets, including two classes.

Table 2. CT image data information

Dataset Name	Covid images	Non-covid images	Total images
COVID-CT dataset	349	397	746
SARS-COV-2	1252	1229	2481

B. Used Techniques

There are two techniques used for the proposed methodology of data preprocessing architecture. These are described one by one in this part.

1) Image Enhancement and Feature Extraction

Image enhancement increases the raw data's quality and informational content before processing. Several levels of compression were utilized to store digitized pictures in this method. GLCM is an excellent discriminator when comparing various images, although this cannot be said for image quality.

Feature Extraction (FE) is vital in any pattern recognition work, particularly in categorizing ultrasonic liver tissues. Ultrasound pictures often exhibit many granular features like texture, and the study of ultrasound images is akin to the challenge of texture analysis. However, the image's textural properties include qualities like smoothness, fitness, & coarseness of a particular pattern. There are several texture feature analysis approaches available. GLCM is employed in this study to extract textural information. GLCM [23] is a second-order statistical approach that relies on (local) information on the gray level between pixels. The matrix is defined over the picture with a specific offset for the distribution of co-occurring values.

From every GLCM, distinct features are retrieved. Consequently, there are seven features for each picture. Before providing features to classifiers, each feature is normalized to fall between 0 & 1, and each classifier gets an identical set of features.

- *GLCM (Gray-Level Co-occurrence Matrix)*

It is a typical technique for defining texture by

analyzing spatial correlation properties of grayscale. Due to the repetitive occurrence of grey distribution in spatial position, there would be a special gray connection among 2 pixels at a given distance, i.e., spatial correlation features of grey in the image. A grayscale histogram is a statistical outcome of a single pixel on the image having a given grayscale; however, GLCM is formed by statistically establishing a state in which 2 pixels divided by a specified distance on the image each have particular grayscale [24].

Take each point (x, y) in the picture (N × N) as well as the point that deviates from it (x + a, y + b) & set the gray value of the point pair to (g1, g2). When a point (x, y) is moved throughout the image, many (g1, g2) values are acquired. K-square describes the sequence of grayscale values and the combination (g1, g2). Count no. of occurrences of each (g1, g2) value & assemble them in a square matrix; next, normalize total no. of (g1, g2) to occurrence probability P (g1, g2); this is referred to as GLCM. Under certain conditions, distance difference values (a, b) may be combined with other variables to produce a joint probability matrix. The texture's periodic distribution defines values (a, b). Finer textures use small difference values like (1, 0), (1, 1), as well as (2, 0); when a = 1 and b = 0, a pixel pair is horizontal, which corresponds to 0° scanning. When a = 0 and b = 1, a pixel pair is vertical, known as 90° scanning. When a = 1 and b = 1, the pixel pair is right diagonal, sometimes referred to as 45-degree scanning. The left diagonal pixel pair corresponds to 135° of scanning when a = -1 and b = 1. This approach transforms (x, y) spatial coordinates to the description of a "gray pair" (g1, g2) based on the likelihood of simultaneous occurrence of two gray levels per pixel, so producing GLCM.

The following is an approach for normalizing GLCM:

$$p(g1, g2) = \frac{p(g1,g2)}{R} \quad (1)$$

The calculation process of R is:

$$R = \begin{cases} N(N-1) & \theta = 0 or \theta = 90 \\ (N-1)^2 & \theta = 45 or \theta = 135 \end{cases} \quad (2)$$

If the picture consists of blocks of pixels with comparable gray values, the diagonal elements of GLCM would have relatively large values; if grey values of image pixels vary locally, the elements that deviate from the diagonal can have larger values.

2) Image Segmentation (IS)

It separates the digital image into distinct regions comprising pixels (also called superpixels) with appropriate attributes. IS aims to transform an image's representation into something more meaningful & easier to study. Typically, IS is utilized to identify objects & boundaries (lines, & curves, etc.) in a picture. IS is a procedure of labelling each pixel in an image such that pixels with the similar label have similar properties. IS is a low-level image processing task aiming to split an image into homogenous regions [25]. Segmentation algorithms depend upon either intensity or discontinuity, or similarity. The first category is to split images depending upon tiny variations in intensity, like edges. 2nd category depends upon splitting the picture into comparable sections depending on a predetermined criterion.

Image segmentation categorizes images into distinct groups [26][27]. Numerous types of research have been performed in image segmentation utilizing clustering. K-Means clustering technique is the most well-known approach.

- *K-means clustering*

The clustering of a picture is the most effective image segmentation method. After extracting features, they are grouped into well-separated clusters depending on each image class. The objective of the clustering method is to generate partitioning decisions depending upon an initial set of clusters that is updated after every iteration. [28].

K-means is an effective approach for clustering. Based on initial cluster centroids, it is utilized to split related data into groups. This algorithm first selects k data values as initial cluster centres, then calculates the distance among every cluster center & every data value and assigns it to the nearest cluster, updates averages of each cluster, and repeats until the condition is no longer satisfied. K-means clustering aims to split data into k clusters where every data value belongs to the cluster with the closest mean [29].

The algorithm for k-means (see in algorithm1), where every cluster's center is denoted by the mean value of objects in a cluster [30].

Algorithm1: K-Means Algorithm

Input: k: No. of clusters.
D: Dataset containing n objects.
Output: A set of k clusters.

Method:

Step 1. Select at random k objects from D to serve as first cluster centers.
Step 2. Repeat
Step 3. Re (assign) every object to the cluster to which it is most closely related depends upon the mean value of objects in the cluster, using the following formula.
Step 4. Determine the average value of every cluster's objects and update cluster means.
Step 5. Until no change.

$$J = \sum_{n=1}^{j} \sum_{m=1}^{i} \left\| X_m^{(n)} - C_n \right\|^2 \quad (3)$$

Where, $\left\| X_m^{(n)} - C_n \right\|^2$ is a calculated distance (intra) between data point X_m m as well as the cluster center C_n, it indicates the distance between the cluster center and their n data points.

Intra term is employed to quantify the density of clusters.

Inter-term represents a minimal distance between cluster centroids.

V. Methodology

The problem definition and technique are presented in detail in the next sections.

A. Problem Specification

Pre-processing [31] is essential due to noisy, inconsistent, and incomplete data. It is one of the preliminary procedures required to achieve high step precision. In the case of radiology images, extraneous features or picture regions degrade the model's performance. As a result, determining ROI (Region of Interest) is the most significant step before the training stage.

B. Proposed Methodology

To achieve the objective of preprocessing medical imaging data for better classification and detection of respiratory disease infection in the human body before applying the Machine learning approaches. This work uses a preprocessing architecture to perform radiological image preprocessing to get enhanced images. At first of this, data acquisition is performed in which two different x-ray & CT scan image datasets are gathered from Kaggle sources. These images are then converted into grayscale images, and the Requantiziation of grey level pixels is used, which is necessary to speed up the computation of feature extraction. These images are resized to get uniformity in the dataset because each image has its dimensions. After this process, an image enhancement technique is applied to speed up the preprocessing of radiology images and locate the Region of Interest (ROI), which is considered pixel association, distance, and direction between pixels. In the automation of radiology image processing, Feature extraction and grouping of extracted feature values improvise the identification of ROI. Thus, GLCM is utilized in the medical industry for feature extraction. These GLMC methods extract from the GLCM matrix properties like Energy, Contrast, Homogeneity, Correlation, Variance, and Entropy. The next task is to apply the k-means clustering approach to photos to conduct segmentation. K-means clustering makes two clusters, one for Foreground Bright Area and the other one for Background Dark Area. Images are segmented by the processing of the k-means clustering technique. Finally, enhanced and segmented images are obtained due to preprocessing mechanism.

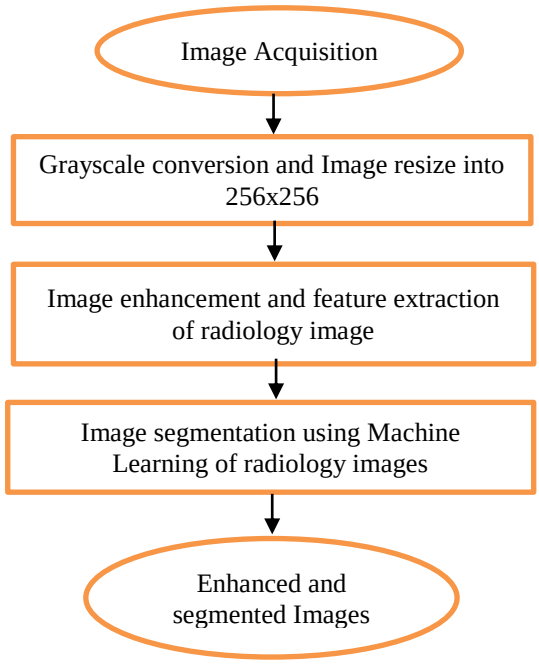

Fig. 5. Proposed flow diagram of preprocessing of radiology images

Figure 5 displays the proposed flow diagram for preprocessing of radiology images. The preprocessing architecture mainly consists of two phases: image enhancement and image segmentation, followed by color conversion and image resizing. The steps for the preprocessing architecture are described below:

Step 1: Image Acquisition Phase

It is an initial step in gathering radiology images. 1st stage of the methodology begins with taking a set of X-ray images & CT images (infected & non-infected) from the available database at [32][33]. Table 3 represents the total images for both datasets.

Table 3. Total images

Radiology images	Instances
X-ray images	6432
CT images	2481

The picture obtained is in its raw format. An abundance of noise is detected in the acquired picture. It must be preprocessed to enhance contrast transparency and background noise separation.

Step 2: Grayscale color conversion and image resizing

However, the collected images are in a Grayscale image. Still, these images are considered RGB color images when processed, so Grayscale color conversion performs on these images to change the color.

In the gathered dataset, the pictures comprise digital scans of printed CT exams & x-ray images; also, there is no standard for the size of the image (the smallest image in the collection has dimensions of 104 by 153 pixels, while the biggest image has dimensions of 484 by 416 pixels). In addition, this dataset lacks standards for image contrast. So, there was a need to resize the images. Therefore, image resizing is performed to standardize the dataset and images are resized into 256x256 pixels.

Step 3: Image enhancement and feature extraction of radiology images

The proposed method depends upon the concept of association between adjacent pixels. Linear dependency is the most basic type of dependency, and the proposed method considers linear dependency of neighboring pixels of a given kernel window size. Features are extracted for important pixels and given to all pixels in their surrounding using a weight matrix, reducing the overall computation time during the image feature extraction. In this case, the feature vector for each non-key pixel is the weighted sum of the feature vectors for all weighting kernel windows that include that pixel. To put it another way, we calculate GLCM features for key pixels & estimate GLCM features for the other pixels using interpolation, which speeds up the calculation & minimizes computation time.

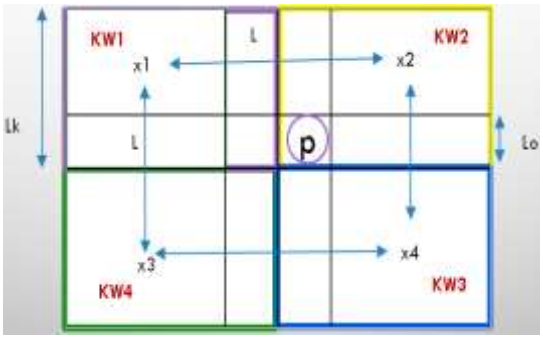

Fig. 6. Four Lk×Lk weighting kernel windows

Figure 6 depicted 4 Lk×Lk weighted kernel windows (Kwi) with a Lo-length overlap. Here, pixel p's features are the weighted sum of those of pixel xi.

$$f(p) = \sum_{i=1}^{n} ai(p) f(xi) \quad (4)$$

where,

f(p)= feature vector of non-key pixel p
xi = is the key pixel located at the center of each of the overlapping weighting windows, which include p;
ai(p) = weight associated with pixel p in the weighting window centered at xi

Step 4: Unsupervised segmentation and clustering of radiology images

Unsupervised Machine Learning is then used to segment the extracted features. For this purpose, perform clustering using K-means and segment the images. Image segmentation aims to transform an image's representation into something more expressive and simpler to analyze. These pixels with similar properties are clustered together in image segmentation.

Inputs consist of k & training data of various classes, where k is no. of clusters. Find centroids of various classes independently; that is, if a collection of points consists of x1, x2,..., xn, then

$$Centroid\ C_j(a) = \frac{1}{n}\sum X_i(a) \quad for\ a = 1,2,\dots\dots d \quad (5)$$

Find the nearest centroid to every point xi via Euclidean Distance (ED). ED: If p = (p1, p2,..., pn) & q = (q1, q2,..., qn) is 2 points in euclidean space, then distance (d) from p to q, or from q to p, may be calculated as follows:

$$d(p,q) = d(q,p)$$
$$= \sqrt{(q1-p1)^2 + (q2-p2)^2 + \cdots + (qn-pn)^2}$$
$$= \sqrt{\sum_{i=1}^{n}(qi-pi)^2} \quad (6)$$

Every point is assigned to the cluster whose mean has Least Squared Euclidean Distance (LSED), the closest mean. A repeat of a similar procedure until clusters are created for every iteration.

Allocate every point to a cluster whose mean has the LSED; this is a cluster with the closest mean [34]. Repeat the same technique until clusters are generated for each iteration. IS in computer vision is segmenting a digital image into several parts (collection of pixels, also called superpixels). The purpose of segmentation is to reduce and/or modify an image's representation to make it more meaningful and accessible for further analysis. The most common use of IS is detecting boundaries (lines, curves, etc.) and objects in images. Image labelling for IS ensures that similarly labelled pixels have similar features. IS creates a set of image-spanning segments or a collection of extracted image contours. Each pixel inside an area has a similar feature or calculated property, like color, intensity, or texture. Significant differences exist across neighbouring areas about the same feature. Clustering is the process of organizing samples such that samples within every group are comparable.

C. Proposed Algorithm

The proposed implementation strategy for the proposed model is described in algorithm 2 below.

Algorithm : RDD_ROI

Input: Radiology images datasets (X-ray images & CT images)
Output: Enhanced and segmented radiology Images

Steps:

Step 1. Input radiology images datasets
Step 2. Transform the input image into a grayscale image

Step 3. Requantize Grayscale Image
Step 4. Image resizing into 256X256
Step 5. Characterize texture of picture using the GLCM method
Step 6. Generate Feature Matrices for the key pixel value of specified Kernel Windows size
Step 7. Extract features like Correlation, Contrast, Homogeneity, Energy, Variance, & Entropy, are features extracted from GLCM matrices
Step 8. Repeat steps 3 to 5 for remaining neighboring key pixels at a distance L
Step 9. Calculate weight associated with non-key pixels
Step 10. Select no. of clusters that correspond to k. For the proposed algorithm, K=2 is considered.
  a. Cluster 1=Foreground Bright Area
  b. Cluster 2= Background Dark Area
Step 11. Allocate data points at random to any of the k clusters.
Step 12. Next, compute the clusters' centers.
Step 13. Compute the distance between every data point and the cluster's center.
Step 14. Based on the distance between every data point and cluster, reassign data points to clusters closest to them.
Step 15. Calculate the new center of the cluster once again.
Step 16. Repeat steps 9, 10, & 11 until data points no longer alter clusters or until the allotted number of iterations has been reached.

Output: Enhanced and segmented radiology images.

VI. Results and Analysis

The experiments have been done using python programming. In result analysis, typical CT scans & CXR images have been compared for Covid-19 affected people. This section has displayed the results of preprocessed image data for each class of different collected image data.

A. Statistics Features

This study retrieved homogeneity, correlation, dissimilarity, contrast, entropy, energy, and ASM from X-ray & CT images. These statistics give information on an image's texture [35][36]. The statistics are shown in table 1 below.

Table 4. Features of Statistics

Statistic	Description
Contrast	Determines the local variances of GLCM.
Correlation	Determine the joint probability of the supplied pixel pair occurrence.
Energy	Offers sum of squared GLCM elements. Additionally, named uniformity & 2nd instant of angle.
Dissimilarity	Distance between object pairs (pixels) in ROI.
Homogeneity	Determines the proximity of GLCM element distribution to GLCM diagonal.
ASM	Image homogeneity measurement
Entropy	Randomness statistics may be employed to define an image's texture.

1) Contrast: It is a measurement of the contrast in intensity between a pixel and its neighbour throughout the whole picture. The contrast is 0 for a "constant" picture (one with no changes).

$$\text{Contrast} = \sum_i \sum_j |i-j|^2 \, p(i,j) \quad (7)$$

2) Homogeneity: Local homogeneity evaluates the proximity of GLCM element distribution to the GLCM diagonal. Homogeneity is 1 for diagonal GLCM.

$$\text{Homogeneity} = \sum_i \sum_j \frac{1}{1+|i-j|^2} p(i,j) \quad (8)$$

3) Correlation: It measures how closely connected each pixel is to its neighbour throughout the whole picture. It's -1 or 1 for an image, i.e., entirely positively or negatively correlated, and infinity for a constant image.

$$\text{Correlation} = \sum_i \sum_j \frac{(i-\mu_i)(j-\mu_j)\, p(i,j)}{\sigma_i \sigma_j} \quad (9)$$

4) Dissimilarity: Distance between pairs of objects (pixels) in ROI is measured by dissimilarity.

$$\text{Dissimilarity} = \sum_i \sum_j |i-j| p(i,,j) \quad (10)$$

5) Entropy: It is a statistical measure of randomness that may be employed to describe an image's texture.

$$\text{Entropy} = \sum_i \sum_j p(i,,j) \log p(i,j) \quad (11)$$

6) Energy: In the GLCM, energy represents the sum of squared components. Its values range from 0 to 1.

$$Energy = \sum_{i,j} P(i,j)^2 \quad (12)$$

7) ASM (Angular Second Moment): It indicates the uniformity of grey level distribution in a picture.

$$ASM = \sum_i \sum_j P(i,j)^2 \quad (13)$$

ASM varies from $1/G^2$ and 1. A value of 1 represents a constant picture.

B. Results

This section illustrates the various experimental outcomes for the improved and segmented x-ray and CT scan image datasets. These results contain several graphs and tables to present the features in the output image compared to the original image concerning Covid effects from both types of image datasets.

1) Results of X-ray images

This subsection is talked about the results for preprocessing results after applying the proposed technique to X-ray images.

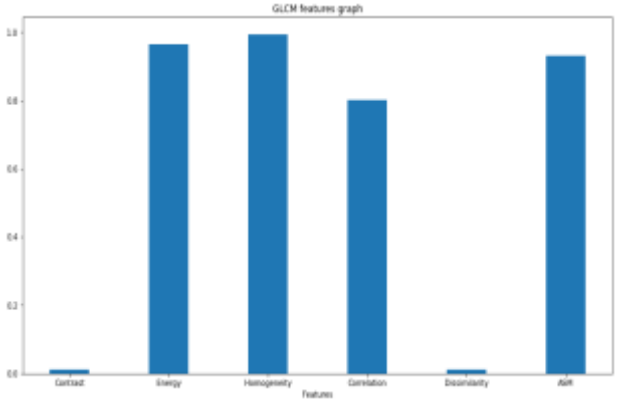

(a) Pneumonia

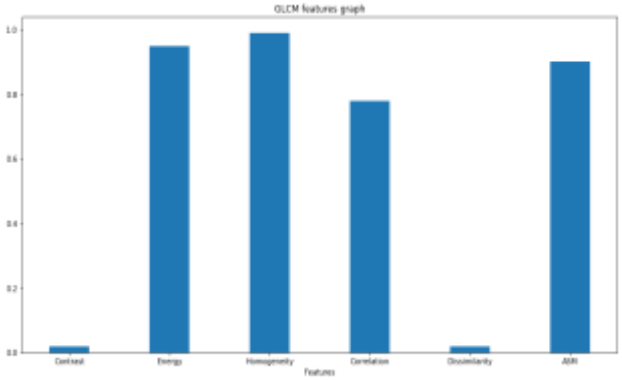

(b) Covid

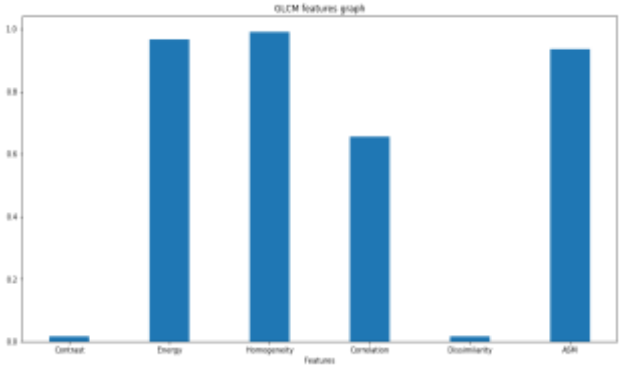

(c) Normal

Fig. 7. GLCM features representations for X-ray images

Figure 7 shows the bar graph for feature value representation in the GLCM method, including pneumonia, covid and normal images. This representation shows that energy, homogeneity and ASM have obtained 100% results. Here, homogeneity is evident. 100% closeness of distribution of elements in GLCM & 100 percent ASM indicates the most uniform grey level distribution in the picture. Also, energy is highest, but the correlation is slightly minimized value. Apart from these, contrast and similarity features have very minimal values in GLCM for all three classes of images.

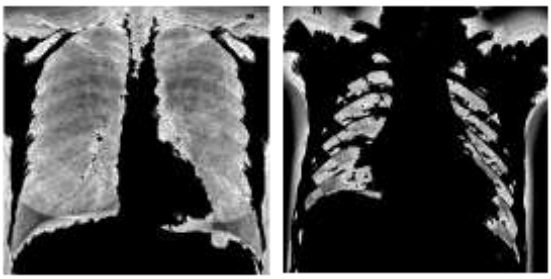

(a) Covid images(b) Pneumonia images

(c) Normal images

Fig. 8. Enhanced image after GLCM feature extraction on x-ray images

Figure 8 displays the enhanced images after applying the image resizing in gray-level images and the GLCM method on x-ray images. In this dataset, pictures comprise digital scans of printed x-ray exams with better image size and quality (every image in the dataset has consistent dimensions of 256 by 256 pixels). Fig. 8 shows some examples of all three classes for enhanced images.

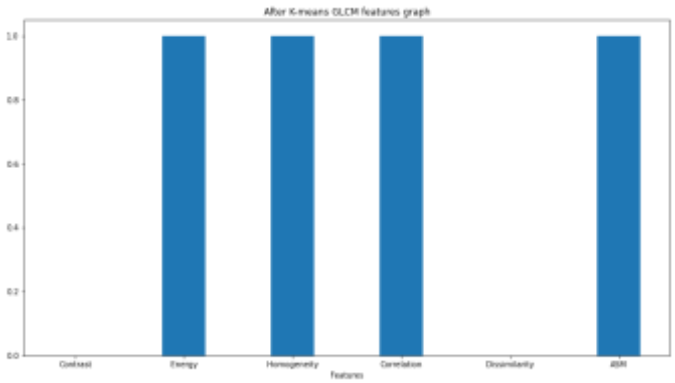

(a) Pneumonia

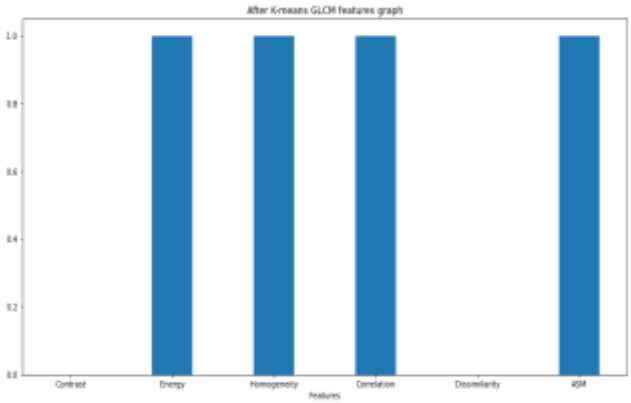

(b) Covid

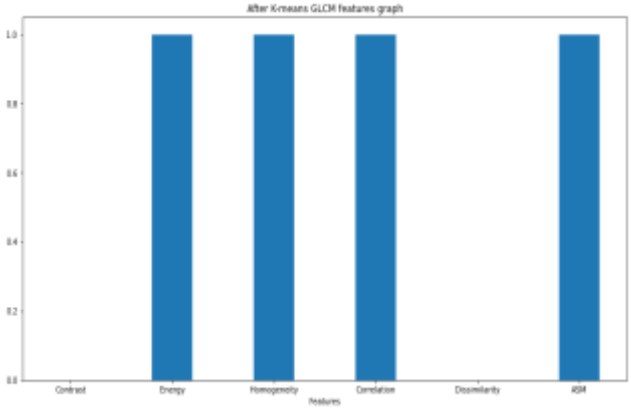

(c) Normal

Fig. 9. GLCM & K-means feature representations for X-ray images

Figure 9 shows the bar graph for feature value representation in proposed techniques, including GLCM & k-means clustering method, pneumonia, covid and normal images for x-ray images. This graphical representation found that energy, homogeneity, correlation and ASM obtained 100% results. These 100% results for all four features show highly distributed closeness in elements, uniform distribution with the highest energy and correlation between pixel to its neighbour over the whole image in GLCM for all three classes of images. But the contrast and dissimilarity have no value in the present contrast intensity of pixels and no distance between pairs of pixels in RoI.

(a) Covid images(b) Pneumonia images

(c)
Normal images

Fig. 10. Segmented image after GLCM & K-means clustering feature extraction on x-ray images

Figure 10 displays the segmented images after applying the proposed preprocessing mechanism, including GLCM and K-means clustering method in gray-level x-ray images, including Covid, pneumonia & normal images. These images display the segmented area based on two clusters for the bright foreground area (cluster 1) and background dark area (cluster 2). In this figure, a bright area displays the chest area, and a dark area displays the background of x-ray images for covid detection out of three classes.

Table 5. Comparative analysis of input image with other techniques for pneumoniaX-ray images

Image Feature	Original Image	GLCM Image	Proposed Technique Image
Contrast	7.1431	1.1459	0.0
Energy	39.9964	96.4990	100.0
Homogeneity	96.5361	99.4270	100.0
Correlation	98.7512	80.0595	100.0
Dissimilarity	6.9533	1.1459	0.0
ASM	15.9972	93.1205	100.0
Entropy	3.0117	0.2640	-0.0

Table 5 represents the comparative analysis for the pneumonia class of the X-ray images dataset based on different image features. This comparison has been put up among original image features after the GLCM method, and the last proposed technique (GLCM and K-mean clustering) image features results. The original image has the highest features value than the GLCM image features. But proposed technique-based image features having 100% results in Energy, Homogeneity, Correlation and ASM features.

Table 6. Comparative analysis of input image with other techniques for COVID X-ray images

Image Feature	Original Image	GLCM Image	Proposed Technique Image
Contrast	7.6852	1.7826	0.0
Energy	45.6089	94.9608	100.0
Homogeneity	96.2712	99.1087	100.0
Correlation	97.0754	77.9210	100.0

Dissimilarity	7.4911	1.7826	0.0
ASM	20.8016	90.1756	100.0
Entropy	2.6279	0.3563	-0.0

Similarly, table 6 represents the comparative analysis for the Covid class of X-ray images dataset based on different image features. This table shows that GLCM image features have the lowest value of contrast, correlation, dissimilarity and entropy than original image features. In contrast, energy, homogeneity and ASM feature value are high and also, using proposed techniques, these features achieved 100% results for covid images effects on the x-ray image.

Table 7. Comparative analysis of input image with other techniques for normal X-ray images

Image Feature	Original Image	GLCM Image	Proposed Technique Image
Contrast	10.9675	1.6722	0.0
Energy	36.6909	96.6993	100.0
Homogeneity	94.6477	99.1639	100.0
Correlation	98.2611	65.5072	100.0
Dissimilarity	10.7339	1.6722	0.0
ASM	13.4622	93.5077	100.0
Entropy	3.3035	0.2602	-0.0

Similarly, table 7 represents the comparative analysis for the normal class of X-ray images dataset based on different image features. This table shows that GLCM image features have the lowest value of contrast, correlation, dissimilarity and entropy than original image features. In contrast, energy, homogeneity and ASM feature value are high, achieving 96.69%, 99.16% and 93.50%, respectively, and also using the proposed technique, these features (energy, homogeneity, correlation and ASM) achieved 100% results for normal images effects on the x-ray image.

Table 8. Final results of an input image with output image forX-ray images of covid

Image Feature	Original Image	Output Image
Contrast	7.1431	0.0
Energy	39.9964	100.0
Homogeneity	96.5361	100.0
Correlation	98.7512	100.0
Dissimilarity	6.9533	0.0
ASM	15.9972	100.0
Entropy	3.0117	-0.0

Table 8 represents the final resulting feature values for the Covid effect analysis on covid x-ray images between the original image & output enhanced segmented image based on different image features. These results found that original image features values varied from 3% to 99%, where correlation features have the highest feature value, i.e., 98.75%, which shows us the highest relation of pixels with its neighbor. When seeing output image features, then found that energy, homogeneity, Correlation and ASM features value achieved 100% results using the proposed techniques. These features will be useful to feed into the classification model, so these features are important for covid images' effects on x-ray images.

2) Results of CT scan images

This section discusses the preprocessing results after applying the proposed technique to CT scan images.

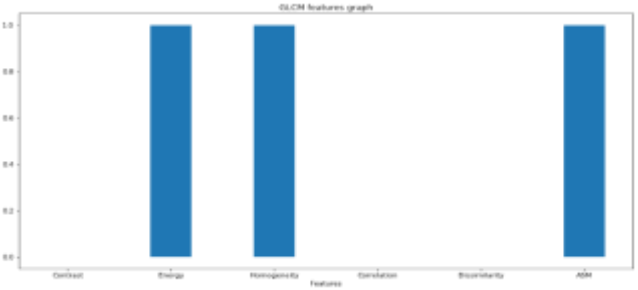

(a) Covid

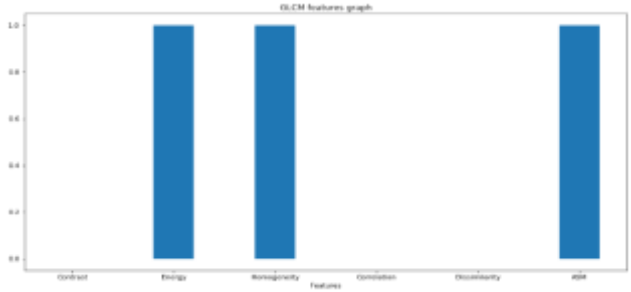

(b) Non-Covid

Fig. 11. GLCM features representations for CT scan images

Figure 11 displays the bar graph plot for feature value representation in the GLCM method, including Covid and non-covid images. This representation shows that energy, homogeneity and ASM have obtained 100% results. The homogeneity shows that 100% closeness of distribution of elements in GLCM and 100% ASM means having the highest uniformity distribution of grey level in the image with 100% energy. But the contrast, correlation and dissimilarity features have no values in GLCM for all two classes of images, which means there is no high contrast in the pixels, no correlation among pixels, and no distance between pairs of pixels in images.

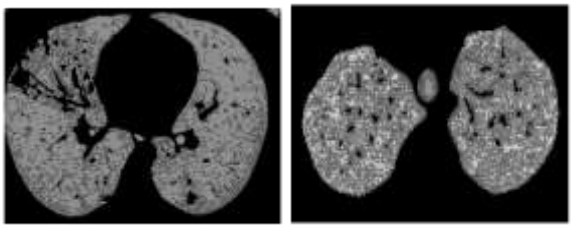

(a) Covid images (b) Non-Covid images

Fig. 12. Enhanced image after GLCM feature extraction on

CT scan image

Figure 12 displays the enhanced images after applying the GLCM method in gray-level images on CT scan images, including non-covid & covid images. In this dataset, images comprise digital scans of printed CT scans and enhanced image quality. Fig. 12 shows some examples of both classes for enhanced images.

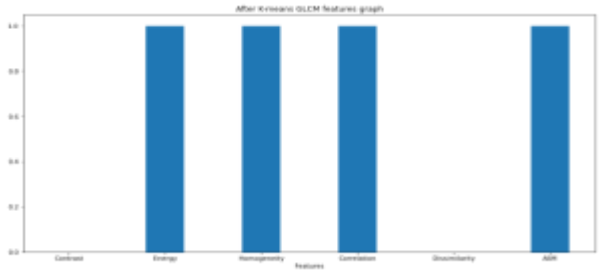

(a) Covid

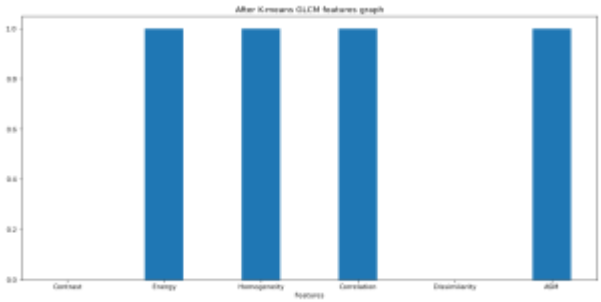

(b) Non-Covid

Fig. 13. GLCM & K-means feature representations for CT scan images

Figure 13 shows the bar graph for representing the feature value in proposed techniques, including GLCM & k-means clustering method for covid & non-covid images for CT scan images. This representation found that energy, homogeneity, correlation and ASM obtained 100% results. This 100% result for all four features shows highly distributed closeness between elements, highly uniform distribution with 100% energy and correlation between pixel to its neighbour over the entire image in GLCM for all three classes of images. But the contrast and dissimilarity have no value representation to present pixels' contrast intensity and not much distance between pairs of pixels in ROI.

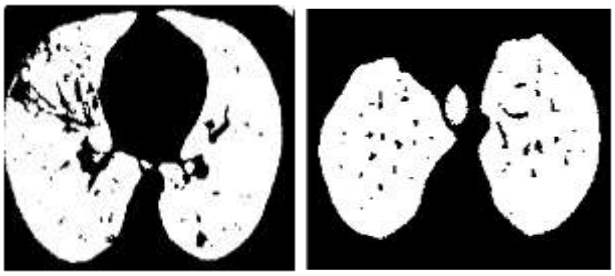

(a) Covid images (b) Non-Covid images

Fig. 14. Segmented image after GLCM & K-means clustering feature extraction on CT scan image

Figure 14 displays the segmented images after applying the GLCM and K-means clustering method in gray-level images on CT scan images, including covid & non-covid images. These images are generated based on two clusters for the bright foreground area (cluster 1) and background dark area (cluster 2). In this figure, a bright area displays the chest area, and a dark area displays the background of CT images for covid & non-covid detection. The segmented area of chest images is visible in this figure.

Table 9. Comparative analysis of input image with other techniques for Covid CT images

Image Feature	Original Image	GLCM Image	Proposed Technique Image
Contrast	31.3704	0.0022	0.0
Energy	51.5728	99.9978	100.0
Homogeneity	88.4653	99.9989	100.0
Correlation	96.4297	-0.0011	100.0
Dissimilarity	24.4273	0.0022	0.0
ASM	26.5976	99.9955	100.0
Entropy	2.7149	0.0004	-0.0

Table 9 represents the comparative analysis for the Covid class of CT images dataset based on different image features. This table shows that GLCM image features have the lowest value of contrast, correlation (in the negative), dissimilarity and entropy than original image features. In contrast, energy, homogeneity and ASM feature value are high, achieving more than 99% results. Still, using proposed techniques, these features achieved 100% results for covid images effects on CT images.

Table 10. Comparative analysis of input image with other techniques for Non-Covid CT images

Image Feature	Original Image	GLCM Image	Proposed Technique Image
Contrast	24.5361	0.0050	0.0
Energy	49.2557	99.9950	100.0
Homogeneity	90.6547	99.9975	100.0
Correlation	97.6214	-0.0024	100.0
Dissimilarity	19.6488	0.0050	0.0
ASM	24.2612	99.9900	100.0
Entropy	2.7065	0.0008	-0.0

Also, Table 10 represents the comparative analysis for the non-Covid class of CT images dataset based on seven different image features in GLCM and k-means clustering. From this table, it can be seen that GLCM image features have less than 0.5% features value of contrast, correlation (in negative value), dissimilarity and entropy than original image features. In contrast, energy, homogeneity and ASM feature value are high, achieving 99.99% results. Still, when applying proposed preprocessing techniques on these features, this achieved 100% results of energy, homogeneity, correlation and ASM features for non-covid

images effects on CT images.

Table 11. Final results of an input image with output image forCT images for covid

Image Feature	Original Image	Output Image
Contrast	31.3704	0.0
Energy	51.5728	100.0
Homogeneity	88.4653	100.0
Correlation	96.4297	100.0
Dissimilarity	24.4273	0.0
ASM	26.5976	100.0
Entropy	2.7149	-0.0

Table 11 represents the final results for the Covid effect on the covid CT images dataset between the original image & output enhanced segmented image based on different image features. These results found that original image features values varied from 2% to 97% before applying image enhancement and segmentation methods where correlation features have the highest feature value, i.e., 96.43%, which shows us the relation between pixels and their neighbor. When seeing output image features, it is then found that energy, homogeneity and ASM feature value achieved 100% results using proposed techniques (GLCM and k-mean clustering). These features achieved 100% results for covid images effects on CT images.

VII. Conclusions & Future Work

This study has designed and processed new preprocessing RDD_ROI architecture to enhance image quality. This architecture consists of image acquisitions, enhancement, feature extraction, and segmentation methods. GLCM method was used to capture features values in a gray level image and texture features from the matrix. Unsupervised Learning K-mean clustering method to extract foreground and background regions. Here, several features in GLCM were calculated to measure the image quality and the feature values were calculated after the proposed architecture for a segmented image. The experiments have been analyzed on the two radiology images datasets of covid (x-ray & CT scan images). The resulting correlation is 100%, which means the images are highly correlated, and dissimilarity is 0, so there are no images that do not have a similarity. Also, the homogeneity and ASM obtained 100% results. The proposed work and experimental results focused on improving the preprocessing of radiology images to detect the spread of respiratory disease. Further, the preprocessed image will be trained to develop an effective technical model for early detection of the spread of respiratory disease infection by using machine learning approaches to benefit society.

Some future research contributions are outlines that can be further implemented to achieve a prediction model of respiratory disease:

1) Analysis and performance measure of the proposed model with proposed preprocessing technique.
2) Creation of a technological model for training a processed radiological picture dataset.
3) Improvised prediction results in the detection of respiratory disease infection.
4) Single technical tool in detecting respiratory disease at an early stage and benefit society.
5) Analysis of respiratory diseases using machine learning techniques.

References

[1] G. Milavetz, “Global Surveillance, Prevention and Control of Chronic Respiratory Diseases: A Comprehensive Approach,” *J. Pharm. Technol.*, 2008, doi: 10.1177/875512250802400215.

[2] S. M. Levine and D. D. Marciniuk, “Global Impact of Respiratory Disease: What Can We Do, Together, to Make a Difference?,” *Chest*, vol. 161, no. 5, pp. 1153–1154, May 2022, doi: 10.1016/j.chest.2022.01.014.

[3] WHO, “World Health Organization. Coronavirus disease 2019 (COVID-19),” *Situat. Report, 32.*, 2020.

[4] M. M. Rahaman *et al.*, “Identification of COVID-19 samples from chest X-Ray images using deep learning: A comparison of transfer learning approaches,” *J. Xray. Sci. Technol.*, vol. 28, no. 5, pp. 821–839, Jul. 2020, doi: 10.3233/XST-200715.

[5] A. Yahiaoui, O. Er, and N. Yumusak, “A new method of automatic recognition for tuberculosis disease diagnosis using support vector machines,” *Biomed. Res.*, vol. 28, no. 9, pp. 4208–4212, 2017.

[6] Z. Hu, J. Tang, Z. Wang, K. Zhang, L. Zhang, and Q. Sun, “Deep learning for image-based cancer detection and diagnosis − A survey,” *Pattern Recognit.*, vol. 83, pp. 134–149, 2018, doi: 10.1016/j.patcog.2018.05.014.

[7] N. E. Dunlap *et al.*, “Diagnostic standards and classification of tuberculosis in adults and children,” *Am. J. Respir. Crit. Care Med.*, vol. 161, no. 4 I, pp. 1376–1395, 2000, doi: 10.1164/ajrccm.161.4.16141.

[8] N. Phukkaphan *et al.*, “Detection of COVID-19 infection based on electronic nose technique: preliminary study,” in *2022 International Electrical Engineering Congress (iEECON)*, 2022, pp. 1–4. doi: 10.1109/iEECON53204.2022.9741576.

[9] S. N. Syed Nor, N. S. Rasanang, S. Karman, W. S. W. K. Zaman, S. W. Harun, and H. Arof, “A Review: Surface Plasmon Resonance-Based Biosensor for Early Screening of SARS-CoV2 Infection,” *IEEE Access*, vol. 10, pp. 1228–1244, 2022, doi: 10.1109/ACCESS.2021.3138981.

[10] S. Devaraj and M. N. Madian, “Deep U-Net Network for identifying Covid 19 infection Using X Ray Images,” in *2020 IEEE International Conference on E-health Networking, Application & Services (HEALTHCOM)*, 2021, pp. 1–5. doi: 10.1109/HEALTHCOM49281.2021.9615913.

[11] R. Anand, S. Fazlul Kareem, R. Mohamed Arshad Mubeen, S. Ramesh, and B. Vignesh, “Analysis Of Heart Risk Detection In Machine Learning Using Blockchain,” in *2021 6th International Conference on Signal Processing, Computing and Control (ISPCC)*, 2021, pp. 685–689. doi: 10.1109/ISPCC53510.2021.9609353.

[12] X. Aggelides, A. Bardoutsos, S. Nikoletseas, N. Papadopoulos, C. Raptopoulos, and P. Tzamalis, “A Gesture Recognition approach to classifying Allergic Rhinitis gestures using Wrist-worn Devices : a multidisciplinary case study,” in *2020 16th International Conference on Distributed Computing in Sensor Systems (DCOSS)*, 2020, pp. 1–10. doi: 10.1109/DCOSS49796.2020.00015.

[13] X. Mei *et al.*, “RadImageNet: An Open Radiologic Deep Learning Research Dataset for Effective Transfer Learning,” *Radiol. Artif. Intell.*, vol. 4, no. 5, 2022, doi: 10.1148/ryai.210315.

[14] G. Litjens *et al.*, “A survey on deep learning in medical image analysis,” *Med. Image Anal.*, vol. 42, pp. 60–88, 2017, doi: 10.1016/j.media.2017.07.005.

[15] V. Cheplygina, M. de Bruijne, and J. P. W. Pluim, “Not-so-supervised: A survey of semi-supervised, multi-instance, and

transfer learning in medical image analysis," *Med. Image Anal.*, vol. 54, pp. 280–296, 2019, doi: 10.1016/j.media.2019.03.009.
[16] S. K. Zhou *et al.*, "A Review of Deep Learning in Medical Imaging: Imaging Traits, Technology Trends, Case Studies with Progress Highlights, and Future Promises," *Proc. IEEE*, vol. 109, no. 5, pp. 820–838, 2021, doi: 10.1109/JPROC.2021.3054390.
[17] X. Liu *et al.*, "A comparison of deep learning performance against health-care professionals in detecting diseases from medical imaging: a systematic review and meta-analysis," *Lancet Digit. Heal.*, vol. 1, no. 6, pp. e271–e297, 2019, doi: 10.1016/S2589-7500(19)30123-2.
[18] E. J. Topol, "High-performance medicine: the convergence of human and artificial intelligence," *Nat. Med.*, vol. 25, no. 1, pp. 44–56, 2019, doi: 10.1038/s41591-018-0300-7.
[19] M. P. Sendak *et al.*, "A Path for Translation of Machine Learning Products into Healthcare Delivery," 2020. doi: 10.33590/emjinnov/19-00172.
[20] M. Roberts *et al.*, "Common pitfalls and recommendations for using machine learning to detect and prognosticate for COVID-19 using chest radiographs and CT scans," *Nat. Mach. Intell.*, vol. 3, no. 3, pp. 199–217, 2021, doi: 10.1038/s42256-021-00307-0.
[21] R. Jain, M. Gupta, S. Taneja, and D. J. Hemanth, "Deep learning based detection and analysis of COVID-19 on chest X-ray images," *Appl. Intell.*, vol. 51, no. 3, pp. 1690–1700, 2021, doi: 10.1007/s10489-020-01902-1.
[22] P. Silva *et al.*, "COVID-19 detection in CT images with deep learning: A voting-based scheme and cross-datasets analysis," *Informatics Med. Unlocked*, vol. 20, p. 100427, 2020, doi: 10.1016/j.imu.2020.100427.
[23] M. Liang and P. Malm, "3D co-occurrence matrix based texture analysis applied to cervical cancer screening," in *Department of Information Technology*, 2012, vol. Master in, p. 35. [Online]. Available: http://www.teknat.uu.se/student%0Ahttp://uu.diva-portal.org/smash/record.jsf?pid=diva2%3A551578&dswid=-1872
[24] P. Shan, "Image segmentation method based on K-mean algorithm," *EURASIP J. Image Video Process.*, vol. 2018, no. 1, p. 81, 2018, doi: 10.1186/s13640-018-0322-6.
[25] P. Panwar, G. Gopal, and R. Kumar, "Image Segmentation using K-means clustering and Thresholding Image Segmentation using K-means clustering and Thresholding," *Int. Res. J. Eng. Technol.*, vol. 3, no. 5, pp. 1787–1793, 2016.
[26] M. K. Jalagam, R. Nanda, R. Rath, and G. Rao, "Image Segmentation using K-means Clustering," *J. Adv. Sci.*, pp. 3700–3704, 2020.
[27] N. Dhanachandra, K. Manglem, and Y. J. Chanu, "Image Segmentation Using K-means Clustering Algorithm and Subtractive Clustering Algorithm," *Procedia Comput. Sci.*, vol. 54, pp. 764–771, 2015, doi: 10.1016/j.procs.2015.06.090.
[28] A. Chitade and S. Katiyar, "Color based image segmentation using K-means clustering," *Int. J. Eng. Sci. Technol.*, vol. 2, 2010.
[29] N. Shi, X. Liu, and Y. Guan, "Research on k-means clustering algorithm: An improved k-means clustering algorithm," in *3rd International Symposium on Intelligent Information Technology and Security Informatics, IITSI 2010*, 2010, pp. 63–67. doi: 10.1109/IITSI.2010.74.
[30] S. B. M. Ahamed and K. S. Hareesha, "Dynamic Clustering of Data with Modified K-Means Algorithm," in *International Conference on Information and Computer Networks (ICICN 2012)*, 2012, vol. 27, no. Icicn, pp. 221–225. doi: 10.13140/2.1.4972.3840.
[31] Z. Xing and H. Jia, "Multilevel Color Image Segmentation Based on GLCM and Improved Salp Swarm Algorithm," *IEEE Access*, vol. 7, pp. 37672–37690, 2019, doi: 10.1109/ACCESS.2019.2904511.
[32] P. PATEL, "Chest X-ray (Covid-19 & Pneumonia)," 2020.
[33] E. Soares, P. Angelov, S. Biaso, M. Froes, and D. Abe, "SARS-CoV-2 CT-scan dataset: A large dataset of real patients CT scans for SARS-CoV-2 identification." 2020. doi: 10.1101/2020.04.24.20078584.
[34] F. Jiang, M. R. Frater, and M. Pickering, "Threshold-Based Image Segmentation through an Improved Particle Swarm Optimisation," in *2012 International Conference on Digital Image Computing Techniques and Applications (DICTA)*, 2012, pp. 1–5. doi: 10.1109/DICTA.2012.6411743.
[35] M. O'Byrne, B. Ghosh, V. Pakrashi, and F. Schoefs, "Texture Analysis Based Detection And Classification Of Structure Features On Ageing Infrastructure Elements," *Hal*, pp. 1–6, 2018.
[36] A. D.O, O. J. A, A. A.O, and D. A.O, "Comparative Analysis of Textural Features Derived from GLCM for Ultrasound Liver Image Classification," *Int. J. Comput. Trends Technol.*, vol. 11, no. 6, pp. 239–244, 2014, doi: 10.14445/22312803/ijctt-v11p151.
[37] Prita Patil; Vaibhav Narawade,'Emphasize of Deep CNN for Chest Radiology Images in the detection of COVID",2022 IEEE 7th International conference for Convergence in Technology (I2CT),DOI: 10.1109/I2CT54291.2022.9825370

AUTHOR PROFILE

Prita Patil
Research Scholar,Department of Computer Engineering,Ramrao Adik Institute of Technology, D Y Patil Deemed to be University, India with professional 11 years of solution, design, development and academic experience. She have led multiple complex business transformation projects in life which are delivered as products to the outside world. She has experience working on research-based and innovative projects that are published and recognized at national and international levels. She is instrumental in techno-functional roles executing the projects with a professional approach. Her Area of specialization is Machine Learning and Data Science and having 10 plus technical publications in International Journals/Conferences.

Dr. Vaibhav Narawade
Professor, Department of Computer Engineering,Ramrao Adik Institute of Technology, D Y Patil Deemed to be University, India with professional 20 years of academic experience. Professor Narawade area of expertise includes Wireless Sensor Network, Image Processing, and Data Science. and having 30 plus technical publications in International Journals/Conferences/Book Chapters. In Academics he is a Board of Studies member in Computer Science and Engineering, Information Technology.